

# INVESTIGATING MATERIALS PROCESSING CHALLENGES FOR ULTRA-HIGH TEMPERATURE CERAMICS

*Dominic Pinnisi<sup>a</sup>, Dr. Elizabeth Opila<sup>a</sup>, Dr. Carolina Tallon<sup>b</sup>, Kevin Gjata<sup>b</sup>*

*<sup>a</sup> University of Virginia, Department of Materials Science and Engineering*

*<sup>b</sup> Virginia Polytechnic Institute and State University, Department of Materials Science and Engineering  
Virginia Space Grant Consortium*

*4/9/21*

**Abstract:** Ultra-high temperature hypersonic components require complex geometries, but severe limitations are placed on the geometries that can be produced by current ultra-high temperature ceramic (UHTC) processing methods. Colloidal processing (CP) followed by pressureless sintering has produced near-net shaped UHTC components, but the oxidation behavior of these components has yet to be compared to that of other state-of-the-art UHTC processing methods. This work is focused on providing a comparison between the oxidation behavior of zirconium diboride specimens processed via CP, spark plasma sintering (SPS), and a combination of the two processes. Sintering aids such as carbon black and boron carbide were also incorporated in this study. Sintered samples were oxidized in air at 1500°C for durations of 5 min., 15 min., 30 min., and 60 min. Specific weight gain and oxide thickness were used as metrics for oxidation resistance. The findings of this study show that the combination of CP and pressureless sintering produces specimens with the most favorable oxidation resistance out of the fabrication methods employed.

## Introduction

### UHTCs

Advancements in hypersonic technology pose a need for development of robust materials, such as ultra-high temperature ceramics (UHTCs), that are capable of operating in extreme environments with temperatures exceeding 2000°C. As hypersonic vehicle speeds increase, the stagnation points of airfoils and other regions of interest will need to endure higher temperatures throughout the duration of flight. As of 2007, the list of known materials that exhibited melting temperatures above 3000°C was limited to 15 materials and compounds, many of which are refractory ceramics based on group IV-V transition metal borides and carbides<sup>1</sup>. These materials are commonly known as UHTCs.

UHTCs are a type of refractory material which are brittle, corrosion resistant, and heat resistant. These properties, among

others, make them ideal candidates to be incorporated in hypersonic aerosurfaces. Material candidates for hypersonics must also be resistant to oxidation, as they will inevitably react with atmospheric oxygen. Furthermore, the oxides of the materials being discussed must also exhibit a sufficiently high melting temperature so as to not melt during flight. Other properties that guide the materials selection process include strength, thermal conductivity, thermal expansion, density, fabricability, and cost<sup>2</sup>. Taking all of this into account, the UHTC being considered in this study was ZrB<sub>2</sub>, which has a melting temperature of approximately 3280°C<sup>3</sup>, and a theoretical density of 6.08 g/cm<sup>3</sup>. An obstacle to incorporating ZrB<sub>2</sub> into hypersonic components is the added cost and complexity of the post-sintering machining necessary to produce intricate geometries found in components such as airfoils and rocket nozzles.

## Processing

Sintering occurs when small particles are heated up to temperatures above half of their melting point<sup>4</sup>. Under these conditions, the particles tend to agglomerate and densify until they form a bulk solid. Sintering can occur with or without externally applied pressure. One such method that achieves sintering while applying incredibly high amounts of pressure is spark plasma sintering (SPS), as can be seen in Figure 1. SPS utilizes Joule heating to rapidly heat samples with an applied current. Samples are additionally under an applied pressure, where the rapid heating rates and pressures can densify samples much more rapidly than conventional sintering processes.

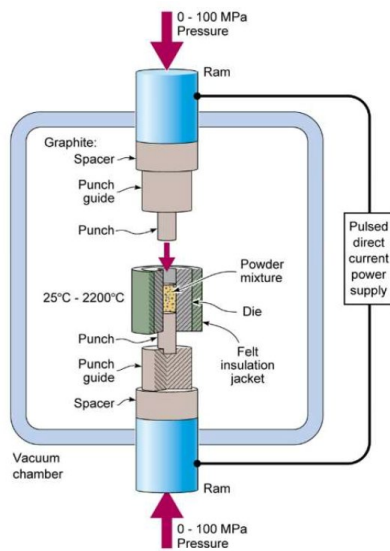


Fig. 1. SPS Diagram (From: UVA Haydn Wadley IPM Lab)

SPS is capable of sintering samples up to nearly 100% theoretical density. This optimized densification is necessary to produce low-porosity components for use in extreme environments like those of hypersonic flight, where oxidation is a design-limiting factor. Yet, SPS results in sample pucks, which need post-processing to be shaped into the required complex

geometries for application. One relatively new fabrication method includes a sequence of colloidal processing (CP) followed by pressureless sintering. CP consists of mixing a ceramic powder with a dispersant and a coagulation agent, and filling a mold of a desired shape with the mixture<sup>5</sup>. A major advantage of this processing method compared to SPS is that it is capable of producing near-net shaped components ideal for hypersonic applications<sup>6</sup>. The CP procedure can be seen in Figure 2.

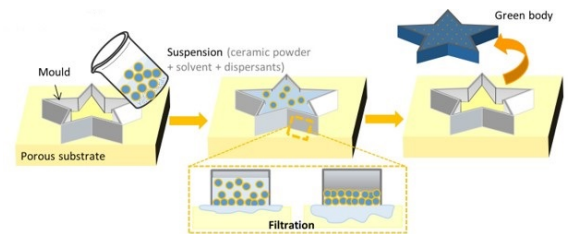


Fig. 2. CP Diagram<sup>7</sup>

Oxidation behavior of samples sintered via colloidal processing and pressureless sintering is well understood<sup>8</sup>, but there has not yet been an accurate comparison to samples that are sintered via state-of-the-art methods under identical conditions. To determine which route is more optimal for producing high-temperature hypersonic components, it is necessary to provide a detailed comparison between oxidation behavior of samples processed by each method. This work seeks to provide a comparison between oxidation resistance of UHTCs processed via colloidal processing in tandem with pressureless sintering, and those processed via SPS.

## Objectives

This work attempted to determine if the oxidation resistance of UHTCs was directly related to the intrinsic properties of the material of choice and the density and microstructure of the component, or if instead the oxidation resistance was affected by

processing techniques, i.e., is there any effect of the use of solvents on the oxidation resistance of UHTCs? To answer this question, the objectives identified for this work were to compare the oxidation resistance of samples produced by each processing method, to observe the effect of incorporating sintering additives in each method, and to quantify the time-dependence of each sample's oxidation behavior. Zirconium diboride ( $ZrB_2$ ) was chosen as the material to be investigated in this project.

### Methods

The investigation under discussion can be broken down into three phases: processing, oxidation, and analysis. Samples of  $ZrB_2$  were colloiddally processed and sintered via pressureless sintering (hereafter referred to as CP+PS) by the Advanced Manufacturing Team at Virginia Tech. CP+PS samples were subsequently shipped to UVA for oxidation testing. Additionally, samples of  $ZrB_2$  were sintered via SPS at UVA. Virginia Tech also produced colloiddally processed green bodies, which were subsequently sintered via SPS at UVA (hereafter referred to as CP+SPS). Cylindrical pucks of approximately 20mm in diameter and 10g in mass were sintered at 2000°C and 65MPa in the case of SPS and CP+SPS, and 2100°C with negligible pressure in the case of CP+PS samples. Prior to oxidation, samples that underwent SPS were cut into rectangular prisms to simplify surface area calculations. Samples that were processed via CP+PS were modeled in Autodesk Inventor Professional due to the aforementioned complexity and time required to machine UHTCs post-processing. Prior to oxidation testing, all samples were cleaned in sequential order: sonicated baths of DI water + detergent, DI water rinse, ethanol, and acetone. After preparation, the sintered samples were placed in a box furnace to oxidize in air at 1500°C for durations of 5

min, 15 min, 30 min, and 60 min. Two oxidation configurations were employed in this study, shown in Figures 3 and 4. The rationale for incorporating an additional and different oxidation configuration will be further explained in the discussion section.

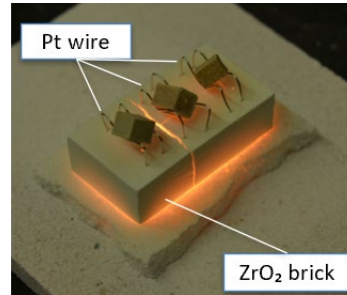


Fig. 3. Oxidation configuration 1 upon removal from a box furnace at 1500°C

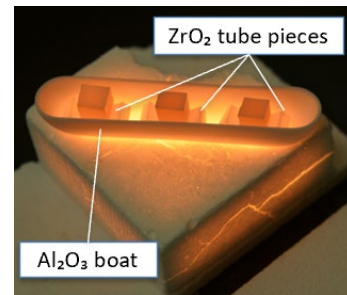


Fig. 4. Oxidation configuration 2 upon removal from a box furnace at 1500°C

After placing the samples in the box furnace at temperature, the time to return to dwell temperature was recorded to identify potential contributions to experimental error from exposure to ambient temperature. After each respective oxidation period, the samples were quickly removed from the furnace and allowed to cool to room temperature in lab air. The specific weight gain (normalized to surface area) of each sample after oxidation was recorded using a high-precision balance. For each sample, the average oxide thickness and microstructure was observed and measured via scanning electron microscopy (SEM). Cross-sectional images were analyzed in ImageJ to measure the oxide thicknesses. Unoxidized samples were also

imaged in SEM to help identify any microstructural changes occurring due to oxidation. Sintering aids such as carbon black (CB) and boron carbide ( $B_4C$ ) were incorporated in this work. Within each of the three different fabrication methods, three different compositions were studied:  $ZrB_2$ ,  $ZrB_2 + 1 \text{ wt\% CB}$ , and  $ZrB_2 + 2 \text{ wt\% } B_4C$ . The incorporation of these sintering aids was based on prior literature<sup>9</sup>.

### Results

The oxidation behavior of each respective sample was characterized by specific weight gain and oxide thickness values. Qualitative analysis of the oxide microstructures resulting from oxidation were also performed on images produced via cross-sectional SEM imaging. The data were plotted in MATLAB, and all plots can be found in Appendix A and Appendix B at the end of this paper. An example of each of these plots is shown in Figures 5 and 6.

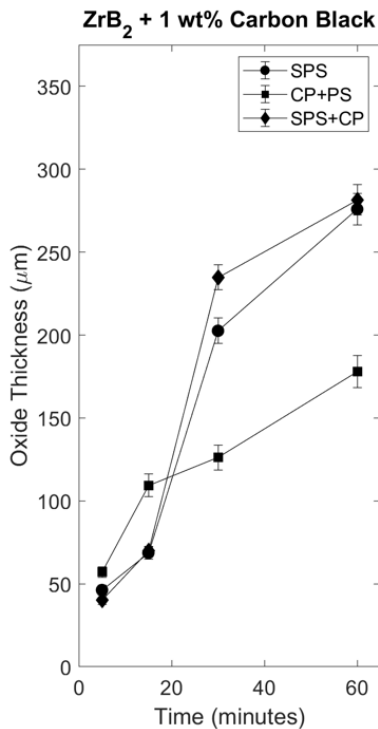


Fig. 5. Oxide Thickness vs. Time for samples with  $ZrB_2 + 1 \text{ wt\% CB}$  composition

For the purpose of retaining clarity in this section, only the plots containing the measured values of the sample which exhibited the best oxidation behavior (on the basis of oxide thickness) will be discussed.

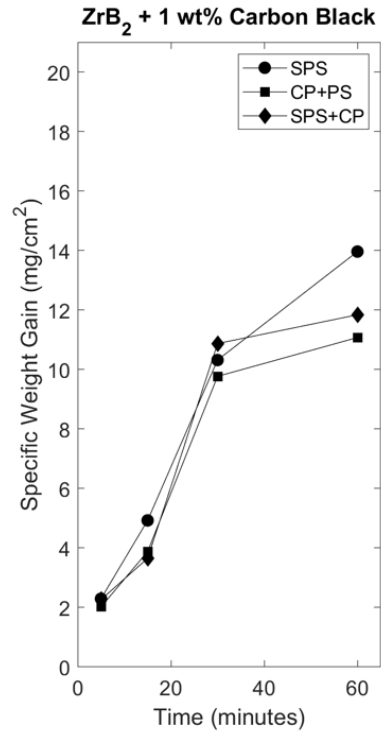


Fig. 6. Specific Weight Gain vs. Time for samples with  $ZrB_2 + 1 \text{ wt\% CB}$  composition

The data in Figures 5 and 6 show that within the  $ZrB_2 + 1 \text{ wt\% CB}$  set of samples, the CP+PS sample exhibited the best oxidation behavior at 60 minutes on the basis of its low oxide thickness and specific weight gain. It is interesting to note that the CP+PS samples actually had the highest oxide thicknesses for the shorter oxidation durations of 5 minutes and 15 minutes, and did not undergo a rapid increase in oxide thickness from 15 minutes to 30 minutes as the SPS and CP+SPS samples did. Additionally, the CP+PS sample shown in Figures 5 and 6 did not have the lowest overall specific weight gain at 60 minutes within the exhaustive set of samples in this study, as can be seen in Appendix A.

The oxide thickness, specific weight gain, density, and % theoretical density can be shown below in Table I for the samples which exhibited the best and worst resistance to oxidation tests of 60 minutes in duration.

**Table I: Oxidation Behavior of Samples Most and Least Resistant to Oxidation**

	Type	Oxide Thickness ( $\mu\text{m}$ )	Specific Weight Gain ( $\text{mg}/\text{cm}^2$ )	Density* ( $\text{g}/\text{cm}^3$ )	% Theoretical Density
ZrB <sub>2</sub>	CP+PS	235.67	12.33	5.46	89.80
	SPS	302.60	17.21	6.06	99.67
ZrB <sub>2</sub> + 1 wt% CB	CP+PS	177.89	11.07	4.98	81.91
	CP+SPS	281.48	11.84	6.04	99.34
ZrB <sub>2</sub> + 2 wt% B <sub>4</sub> C	CP+PS	196.62	6.49	5.72	94.08
	CP+SPS	251.42	9.09	5.84	96.05

1500°C, air, 60 minutes

\* = measured via Archimedes principle

The samples in Table I which exhibited the most favorable oxidation behavior within each composition subset are shown in the highlighted rows. The samples in Table I which exhibited the least favorable oxidation behavior within each composition subset are shown in the unhighlighted rows. Overall, CP+PS ZrB<sub>2</sub> + 1 wt% CB yielded the lowest oxide thickness, but it did not yield the lowest specific weight gain. Additionally, the CP+PS ZrB<sub>2</sub> + 1 wt% CB sample had the lowest density which raises the question of why it was able to be more resistant to oxidation.

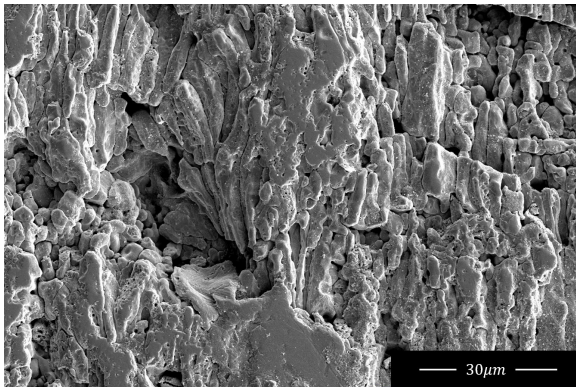


Fig. 7. Cross-section view of CP+PS ZrB<sub>2</sub> + 1 wt% CB (oxidized at 1500°C for 60 min)

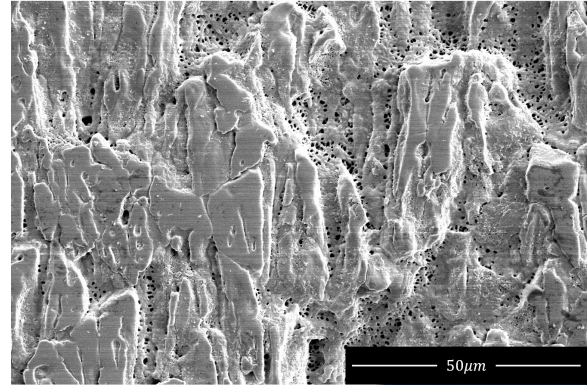


Fig. 8. Cross-Section view of SPS ZrB<sub>2</sub> sample (oxidized at 1500°C for 60 min)

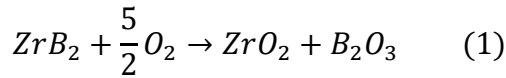
The samples shown in Figures 7 and 8 both display the typical columnar structure of oxidized ZrB<sub>2</sub>. A key difference between the two is that the columnar structure of the SPS ZrB<sub>2</sub> sample appears to be enmeshed in a highly porous structure of unknown composition. Future work will seek to analyze these samples with energy dispersive x-ray spectroscopy to identify the phases present. An additional difference between these two microstructures is that the columnar structures of the CP+PS ZrB<sub>2</sub> + 1 wt% CB sample appear to be smaller in length than those of the SPS ZrB<sub>2</sub> sample.

## Discussion

### Analysis

The results indicate that samples of ZrB<sub>2</sub> with 1 wt% CB that were processed via CP+PS were most resistant to oxidation at longer times despite their significantly lower densities. It remains unclear whether the samples exhibited linear or parabolic oxidation kinetics, as the data fit equally well into both models. In all cases, the samples gained mass with time, and their oxide thicknesses also grew with time. This was expected, as oxygen has a valence of -2, which makes it ideal for reacting with zirconium which has a valence of +4. The oxygen in the ambient furnace air attached

itself to the zirconium atoms in each sample to produce an oxide layer of  $ZrO_2$ . In the case of samples with 2 wt%  $B_4C$  added, the specific weight gains were notably lower. This was expected as  $B_2O_3$  is a byproduct of the oxidation of  $ZrB_2$ , as shown below in Eq. (1).



$B_2O_3$  is known to sublime at temperatures above  $1200^\circ C$ <sup>10</sup>, which is likely what led to a lower specific weight gain overall for samples which contained 2 wt%  $B_4C$ . The sublimation of  $B_2O_3$  would also have produced porosity in the oxide layer, which can be seen clearly in Figure 8.

All samples exhibited similar oxidation behavior at lower temperatures (most significantly those with 2 wt%  $B_4C$  added), indicating that the chemical makeup and processing method of the samples did not have a profound effect on their oxidation behavior until they dwelled at temperature for longer durations. This is promising for applications that require minimal operational time, but less promising for applications with longer operational times.

The microstructure of the best and worst material candidates from the 60-minute oxidation subset were similar in that their oxides were both columnar. However, there appeared to be a larger degree of porosity in the  $ZrB_2$  sample produced via SPS, indicating that porosity developed during oxidation serves to accelerate oxygen transport and reduce oxidation resistance.

### Error

As previously mentioned, two oxidation configurations were implemented in this study. Configuration 1 quickly became problematic as samples occasionally reacted with the platinum wire, thus skewing their

overall mass gains. The zirconia bricks used in Configuration 1 were also prone to thermal shocking, making them less-than-ideal for longer duration oxidation tests. For these reasons, Configuration 2 became the primary oxidation configuration for the remainder of this study. There were only 2 regions of contact with the sample holder in both configurations. However, Configuration 2 reduced the air accessible to the downward-facing surface of each sample, further skewing specific weight gain results. These inconsistencies made it evident that specific weight gain could not be used as a primary metric for oxidation behavior, which is why greater emphasis was placed on oxide thickness in this analysis.

Using oxide thickness as a metric is not without flaw either. Before oxidation, samples were machined to near-equal dimensions to the best of the experimenter's ability using a low-speed saw. The aforementioned difficulties of post-processing machining with UHTCs were incredibly evident, and the samples ended up being dimensionally different from one another. The CP+PS samples, which were modeled in Autodesk Inventor Professional, were geometrically irregular as well. A downside to producing geometrically irregular and geometrically different samples is that the oxide thickness varies depending on location around each sample. This made it difficult to truly identify a representative oxide thickness. 30 different measurements were taken on each oxide, and the standard deviation of each set of measurements was within  $\pm 11.8\mu m$ .

### Future Work

Future work which will be completed before the end of Spring 2021 will include analyzing microstructural changes before and after oxidation, and assessing the affect that initial grain size had on the oxidation

behavior of each sample. Future extensions of this work will investigate the oxidation behavior of each sample at higher oxidation durations to provide a better idea of whether the oxidation kinetics are more linear or parabolic. The same trials completed in this experiment should also be repeated using only Configuration 2, or some other configuration which is to remain constant throughout the study without introducing any experimental error through its use. Subsequent studies could also investigate the same properties for a different UHTC such as titanium diboride (TiB<sub>2</sub>).

### Conclusion

The oxidation behavior of ZrB<sub>2</sub> that was fabricated by SPS, CP+PS, and CP+SPS was observed in this study in order to provide a comparison between the three processes. The motivation for this study was driven by the difficulties in processing UHTCs and the potential for incorporating a novel processing technique so long as doing so wouldn't occur at the expense of oxidation behavior. The primary finding of this work is that samples of ZrB<sub>2</sub> mixed with 1 wt% CB that were processed via CP+PS displayed the lowest amount of oxidation out of all samples. This serves to strengthen the claim that CP+PS is a viable alternative to processing UHTCs, which would reduce complexity and costs of manufacturing hypersonic components.

### Acknowledgements

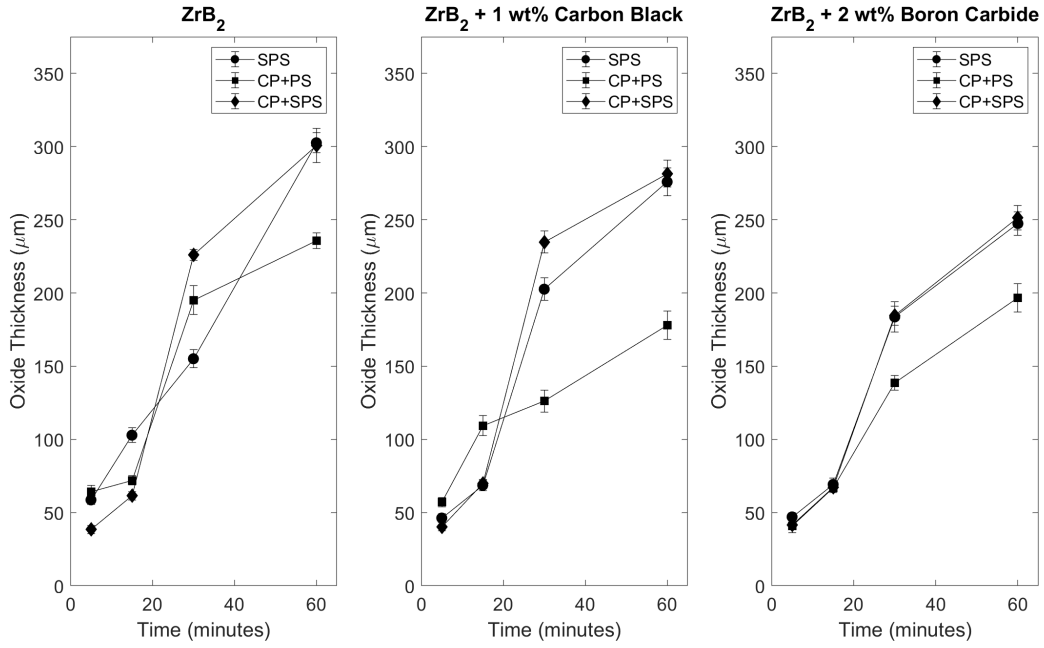
This work was carried out under the guidance of Dr. Elizabeth Opila (UVA) and Dr. Carolina Tallon (VT), in collaboration with Kevin Gjata, a former undergraduate student at Virginia Tech. This work was financially supported by the 4-VA partnership and by the Virginia Space Grant Consortium. This work also relied heavily on facilities and equipment made available by the UVA Nanoscale Materials Characterization Facility.

### References

1. E. Wuchina, E. Opila, M. Opeka, W. Fahrenholtz, I. Talmy, UHTCs: Ultra-High Temperature Ceramic Materials for Extreme Environment Applications, The Electrochemical Society Interface, 2007
2. Cao, G. et. al., Ultra High Temperature Ceramics for Space Propulsion. CESMA, 2016
3. Stanfield, A.D., Manara, D., Robba, D., Hilmas, G.E. and Fahrenholtz, W.G. (2021), Measurement of the melting temperature of ZrB<sub>2</sub> as determined by laser heating and spectrometric analysis. J Am Ceram Soc.
4. J.E. Burke, Sintering and Microstructure Control, Chapter 18 in Chemical and Mechanical Behaviour of Inorganic Materials, 1970
5. Opila, E., Tallon, C., Oxidation Resistance of Ultra-High Temperature Ceramics Fabricated by Novel Processing Routes. University of Virginia and Virginia Polytechnic Institute and State University, 2017
6. C. Tallon, G. Franks, Recent Trends in Shape Forming from Colloidal Processing: A Review, Journal of the Ceramic Society of Japan, 119, p.147-160, 2007
7. Franks, GV, Tallon, C, Studart, AR, Sesso, ML, Leo, S. Colloidal Processing: Enabling Complex Shaped Ceramics with Unique Multiscale Structures. J Am Ceram Soc. 2017; 100: 458– 490.
8. Sung S. Hwang, Alexander L. Vasiliev, Nitin P. Padture, Improved processing and oxidation-resistance of ZrB<sub>2</sub> ultra-high temperature ceramics containing SiC nanodispersoids, Materials Science

- and Engineering: A, Volume 464,  
Issues 1–2, 2007, Pages 216-224,
9. Zhang, S.C., Hilmas, G.E. and  
Fahrenholtz, W.G. (2008),  
Pressureless Sintering of ZrB<sub>2</sub>–SiC  
Ceramics. Journal of the American  
Ceramic Society, 91: 26-32.
  10. T.A. Parthasarathy, R.A. Rapp, M.  
Opeka, R.J. Kerans, A model for the  
oxidation of ZrB<sub>2</sub>, HfB<sub>2</sub> and TiB<sub>2</sub>,  
Acta Materialia, Volume 55, Issue  
17, 2007, Pages 5999-6010

## Appendix A



## Appendix B

